

CT Texture Analysis in Nonalcoholic Fatty Liver Disease (NAFLD)

Laura E. Dichtel^{*,†}, Azadeh Tabari[‡], Nathaniel D. Mercaldo^{*,‡}, Kathleen E. Corey^{*,§}, Jad Hussein^{*,‡}, Stephanie A. Osganian[§], Mark L. Chicote[†], Elizabeth M. Rao[†], Karen K. Miller^{*,†}, Miriam A. Bredella^{*,‡}

^{*}Harvard Medical School, Boston, MA, USA, [†]Neuroendocrine Unit, Massachusetts General Hospital, Boston, MA, USA, [‡]Department of Radiology, Massachusetts General Hospital, Boston, MA, USA and [§]Department of Gastroenterology, Massachusetts General Hospital, Boston, MA, USA

Background: Nonalcoholic fatty liver disease (NAFLD) is the most common form of liver disease worldwide. There are limited biomarkers that can detect progression from simple steatosis to nonalcoholic steatohepatitis (NASH). The purpose of our study was to utilize CT texture analysis to distinguish steatosis from NASH. **Methods:** 16 patients with NAFLD (38% male, median (interquartile range): age 57 (48–64) years, BMI 37.5 (35.0–46.8) kg/m²) underwent liver biopsy and abdominal non-contrast CT. CT texture analysis was performed to quantify gray-level tissue summaries (e.g., entropy, kurtosis, skewness, and attenuation) using commercially available software (TexRad, Cambridge England). Logistic regression analyses were performed to quantify the association between steatosis/NASH status and CT texture. ROC curve analysis was performed to determine sensitivity, specificity, AUC, 95% CIs, and cutoff values of texture parameters to differentiate steatosis from NASH. **Results:** By histology, 6/16 (37%) of patients had simple steatosis and 10/16 (63%) had NASH. Patients with NASH had lower entropy (median, interquartile range (IQR): 4.3 (4.1, 4.8) vs. 5.0 (4.9, 5.2), $P = 0.013$) and lower mean value of positive pixels (MPP) (34.4 (21.8, 52.2) vs. 66.5 (57.0, 70.7), $P = 0.009$) than those with simple steatosis. Entropy values below 4.73 predict NASH with 100% (95%CI: 67–100%) specificity and 80% (50–100%) sensitivity, AUC: 0.88. MPP values below 54.0 predict NASH with 100% (67–100%) specificity and 100% (50–100%) sensitivity, AUC 0.90. **Conclusion:** Our study provides preliminary evidence that CT texture analysis may serve as a novel imaging biomarker for disease activity in NAFLD and the discrimination of steatosis and NASH. (J CLIN EXP HEPATOL xxxx;xxx:xxx)

Nonalcoholic fatty liver disease (NAFLD) is the most common cause of liver disease with a global prevalence of 25%.¹ NAFLD encompasses a spectrum ranging from simple steatosis to nonalcoholic steatohepatitis (NASH). NASH can lead to cirrhosis, decompensated liver disease and hepatocellular carcinoma^{2,3} and is the second leading indication for liver transplantation in the United States and predicted to become the leading indication within the next decade.⁴

Clinical research in NAFLD and NASH has been limited by the lack of validated non-invasive techniques to assess liver steatosis, inflammation and fibrosis. Liver biopsy remains the gold standard for diagnosis of NAFLD, fibrosis

and NASH and is unique in its ability to quantify lobular inflammation and hepatocyte ballooning and exclude secondary causes of liver disease. However, biopsy is invasive and associated with complications such as bleeding and infection,⁵ and subject to potential sampling error.⁶ Thus alternative, non-invasive approaches to liver disease staging are of high priority. Magnetic resonance imaging (MRI) and proton spectroscopy (¹H-MRS)^{7,8} as well as computed tomography (CT)^{9,10} are sensitive imaging modalities for the assessment of hepatic steatosis. Advanced Magnetic resonance (MR) techniques, such as MR elastography^{11,12} or liver multiScan^{13,14} can predict fibrosis in NAFLD but require access to liver MRI and specialized sequences and post-processing. Transient elastography (FibroScan) is a technique that has good predictive accuracy for higher levels of fibrosis and cirrhosis, but it is operator dependent, requires specialized equipment and is limited in patients with obesity.¹⁵ CT texture analysis is an objective approach to quantify gray-level patterns of tissues by using computer-assisted measurements that are independent of subjective visual interpretation.¹⁶ An advantage of CT texture analysis over advanced MR techniques is the potential for opportunistic hepatic assessment on routine abdominal CTs performed for other purposes, which could be prospectively or retrospectively analyzed to detect assess for NAFLD/NASH.

Keywords: nonalcoholic fatty liver disease (NAFLD), nonalcoholic steatohepatitis (NASH), computed tomography, texture analysis

Received: 5.2.2023; Accepted: 4.4.2023; Available online: xxx

Address for correspondence: Miriam A. Bredella, MD, MBA, Massachusetts General Hospital, Yawkey 6E, 55 Fruit Street, Boston, MA, 02114, USA. Tel.: +617 726 7717; fax: +617 726 5282

E-mail: mbredella@mgh.harvard.edu

Abbreviations: AASLD: American Association for the Study of Liver Disease; AUC: area under the curve; MPP: mean value of positive pixels; NAFLD: nonalcoholic fatty liver disease; NAS: NAFLD activity score; NASH: nonalcoholic steatohepatitis; OR: odds ratio; ROC: receiver operator characteristic

<https://doi.org/10.1016/j.jceh.2023.04.001>

Studies have used CT texture analysis in patients with neoplasms to differentiate benign from malignant lesions, assess tumor grade, or predict survival in patients with cancer.^{17,18} Recently, CT texture analysis, using in-house developed programs, has been used to assess hepatic fibrosis in chronic liver disease on contrast-enhanced and non-enhanced CTs; however, these programs are not widely available.^{19,20} In a recent study, Naganawa *et al.*²¹ performed CT texture analysis using a commercially available texture analysis program but were only able to predict NASH in patients without suspicion of hepatic fibrosis based on hyaluronic acid levels. Therefore, additional data is needed that utilize commercially available CT texture programs.^{22,23}

The purpose of our study was to determine CT texture features of the liver using a commercially available texture analysis program to distinguish steatosis from NASH in a group of individuals with concurrent liver histology.

METHODS

Cohort Selection

This is a retrospective cross-sectional study of patients enrolled in an institutional review board-approved and Health Insurance Portability and Accountability Act-compliant natural history study of patients with NAFLD.^{24–26} All subjects provided written informed consent for enrollment into the parent natural history study prior to data collection. The study has been carried out in accordance with The Code of Ethics of the World Medical Association (Declaration of Helsinki). Patients in the repository who had undergone an abdominal CT were assessed for eligibility. Inclusion criteria were diagnosis of NAFLD and the availability of an abdominal non-contrast CT scan and liver biopsy within ± 6 months of each other. A time interval of 6 months was chosen as liver histology is not expected to change if subjects maintain a stable weight and do not undergo procedures or therapy that affects hepatic steatosis. Therefore, weight change between the date of biopsy and date of CT scan was documented. Liver enzymes, aspartate aminotransferase (AST) and alanine aminotransferase (ALT), obtained within 4 weeks of the liver biopsy, were recorded. Exclusion criteria were weight loss surgery or loss of more than 1.5 kg/m² BMI between the CT and biopsy. Additional exclusion criteria included excess alcohol intake (more than two alcoholic drinks per day in women or three in men) or possible drug induced NAFLD with history of chronic oral steroid, methotrexate or tamoxifen use (Figure 1).

Assessment of Liver Histology

Liver biopsies were reviewed by a single blinded hepatopathologist and scored for steatosis grade (0 = < 5%; 1 = 5%–

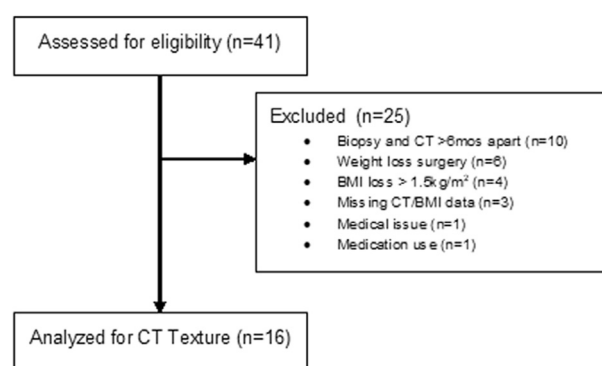


Figure 1 Flow diagram.

33%; 2 = 33%–66%; 3 > 66%), lobular inflammation per 200 \times (0 = no foci; 1 = < 2 foci; 2 = 2–4 foci; 3 = > 4 foci) and hepatocyte ballooning (0 = no ballooning; 1 = few; 2 = many) per Kleiner *et al.* NAFLD activity score (NAS) was then assigned from 0 to 8 as a sum of the steatosis grade, lobular inflammation and hepatocyte ballooning values.²⁷ Fibrosis stage was assessed according to the modified Brunt stage (0–4), with four representing cirrhosis.²⁴ Subjects were then classified as having simple steatosis (n = 6), defined by grade 1 or higher steatosis without ballooning, inflammation or fibrosis, or NASH (n = 10), defined by grade ≥ 1 in steatosis, lobular inflammation and hepatocyte ballooning per the American Association for the Study of Liver Disease (AASLD).²⁸

CT Acquisition

Non-contrast CTs of the abdomen were performed using 64-slice multidetector CT scanners (Light-Speed VCT; GE Medical Systems, Milwaukee, Wisconsin or Somatom Definition; Siemens Medical Solutions, Ann Arbor, Michigan). The following parameters were used: variable tube current (150 mA maximum depending on patient size), 120 kVp, pitch of 1–1.5, rotation time of 0.5–0.8 s, section thickness of 2.5 mm, and standard reconstruction algorithm.

CT Texture Analysis

CT texture analysis was performed by a research instructor with 6 years of experience (A.T.), who was supervised by a fellowship-trained radiologist with 15 years of experience (M.A.B.) using commercially available software (TexRad, Cambridge England). A single circular region of interest in the peripheral portion of the right hepatic lobe was drawn avoiding hepatic vessels. The texture analysis approach includes an initial filtration step to extract and enhance features of different sizes (i.e. fine, medium and coarse texture scales corresponding to 1–4 mm in size) and to reduce noise. The following texture parameters were obtained on 12-bit images (4096 gray-levels); skewness, the asymmetry of gray-level pixel distribution; kurtosis, the pointedness or peakedness of pixel distribution;

Table 1 Patient Demographics and CT Texture Variables by Histology Status.

	Steatosis <i>n</i> = 6	NASH <i>n</i> = 10	<i>P</i>
Demographics			
Age (in years)	50 (27–61)	58 (51–64)	0.28
BMI (in kg/m ²)	47 (42–50)	36 (34–38)	0.03
Female, % (number of subjects)	50% (3)	70% (7)	0.79
AST (in U/L)	35 (8–63)	55 (36–73)	0.23
ALT (in U/L)	40 (17–77)	72 (47–97)	0.14
CT texture features			
Entropy	5.01 (4.92–5.17)	4.31 (4.08–4.82)	0.013
Kurtosis	−0.18 (−0.21–−0.12)	−0.08 (−0.15–−0.04)	0.08
Mean of positive pixels (MPP)	66.5 (57.0–70.7)	34.4 (21.8–52.2)	0.009
Skewness	0.15 (0.04–0.24)	0.09 (0.03–0.14)	0.38

Categorical variables are presented as frequencies and percentages and continuous variables are presented as median and interquartile range (IQR). Abbreviations: BMI, body mass index; AST, Aspartate transaminase; ALT, alanine transaminase; MPP, Mean of positive pixels. *P*-values are derived from the Wilcoxon rank sum and the Fisher's Exact test for continuous and categorical variables, respectively.

entropy, the inhomogeneity of pixel distribution; and mean value of positive pixels (MPP), the average attenuation value of pixels or greater than zero without filter application (Supplementary Figure).^{29,30} CT texture analysis is not currently an FDA-approved technique.

Statistical Analysis

Descriptive summaries were computed by disease group (NASH, steatosis). Categorical variables were summarized as frequencies and percentages, and group differences were assessed using Fisher's exact test. Continuous variables were summarized as median (interquartile range (IQR) = 25th and 75th percentiles), and group differences were assessed using Wilcoxon rank sum test. Box-plots were created to summarize the distribution of each texture variable by disease group.

Separate univariate logistic regression models were constructed to quantify the association between NASH/steatosis status and each texture value (entropy, kurtosis, MPP, and skewness). Both linear and non-linear representations of each texture value was considered, but there was insufficient evidence to justify the more flexible coding of the texture value (via a chunk test). Exponentiated parameter estimates, and their 95% confidence intervals, were calculated to summarize the odds ratio (OR) of having the diagnosis of NASH for each standard-deviation increase in texture score. A receiver operator characteristic (ROC) curve analysis was performed, and the associated area under the ROC curve (AUC) calculated, to quantify the discriminative ability of each texture variable to diagnosis NASH. Estimates, and bootstrapped confidence intervals of sensitivity, specificity, and accuracy were computed for cut-points (or thresholds) along the ROC

curve. The “best” cut-point was defined using Youden's Index (the value that maximizes the average sensitivity and specificity). All analyses were performed using R 4.1.0.³¹

RESULTS

Clinical Characteristics

We included 16 subjects, 10 women, 6 men, median (IQR) age 57 (48–64) years and BMI 38 (35–47) kg/m². By histology, 6/16 (37%) of subjects had simple steatosis and 10/16 (63%) patients had NASH. Of the subjects with NASH, 8/10 (80%) had fibrosis ranging from stage 1a to 4. Differences in the distributions of age were not detected by disease group [median (IQR): 58 (51–64) vs. 50 (27–61) years, *P* = 0.28] but patients with NASH had a significantly lower BMI than those with steatosis only [median (IQR): BMI 36 (34–38) vs. 47 (42–50), *P* = 0.03]. The median time between biopsy and CT was 8 days (IQR 1–57 days). There were no significant differences in liver enzymes between the groups (Table 1).

CT Texture Parameters

Patients with NASH had lower mean entropy [median (IQR): 4.31 (4.08–4.82) vs. 5.01 (4.92–5.17), *P* = 0.013] and lower MPP [median (IQR): 34.4 (21.8–52.2) vs. 66.5 (57.0–70.7), *P* = 0.009] compared to those with simple steatosis. Kurtosis and mean skewness were not significantly different between simple steatosis and NASH groups (*P* = 0.08 and *P* = 0.38, respectively). There was insufficient evidence to conclude the mean skewness distributions differed between disease groups [median (IQR): 0.09 (0.03–0.14) vs. 0.15 (0.04–0.24), *P* = 0.38] (Table 1).

Table 2 Preliminary Diagnostic Summaries by Texture Metric and Threshold Value.

Texture Parameter	Threshold Estimate (95% CI)	Specificity Estimate (95% CI)	Sensitivity Estimate (95% CI)	Accuracy Estimate (95% CI)
Entropy	4.73 (4.54, 4.99)	1.00 (0.67, 1.00)	0.80 (0.50, 1.00)	0.88 (0.69, 1.00)
Kurtosis	-0.10 (-0.17, -0.08)	1.00 (0.67, 1.00)	0.70 (0.40, 1.00)	0.81 (0.62, 0.94)
MPP	54.03 (39.69, 63.66)	1.00 (0.50, 1.00)	1.00 (0.50, 1.00)	0.88 (0.69, 1.00)
Skewness	0.17 (0.01, 0.35)	0.67 (0.17, 1.00)	0.90 (0.50, 1.00)	0.75 (0.56, 0.94)

Abbreviations: Mean of Positive Pixels (MPP). Confidence intervals were calculated using a stratified bootstrap resampling procedure. Bolded entries reflect the “best” threshold using the Youden Index.

Discriminative Ability of Texture Metrics to Differentiate Steatosis from NASH

ROC curve analysis was used to determine threshold values of texture parameters to distinguish steatosis from NASH. Using a threshold of 4.73 (95% CI 4.54–4.99) for entropy resulted in a sensitivity, specificity, and accuracy of 100% (95% CI 0.67–1.00), 80% (95% CI 0.50, 1.00), and 88% (95% CI 0.69,

1.00), respectively, and an AUC of 0.88 (95% CI: 0.72–1.00) (Figure 1 and Table 2). For MPP, using a threshold of 54, the sensitivity, specificity, and accuracy were 100% (95% CI 0.50–1.00), 100% (95% CI 0.50–1.00), and 88% (95% CI 0.69–1.00), and an AUC of 0.90 (95% CI 0.74–1.00) (Figure 2 and Table 2). Accuracy and AUC for the other texture parameters are summarized in Figure 2 and Table 2.

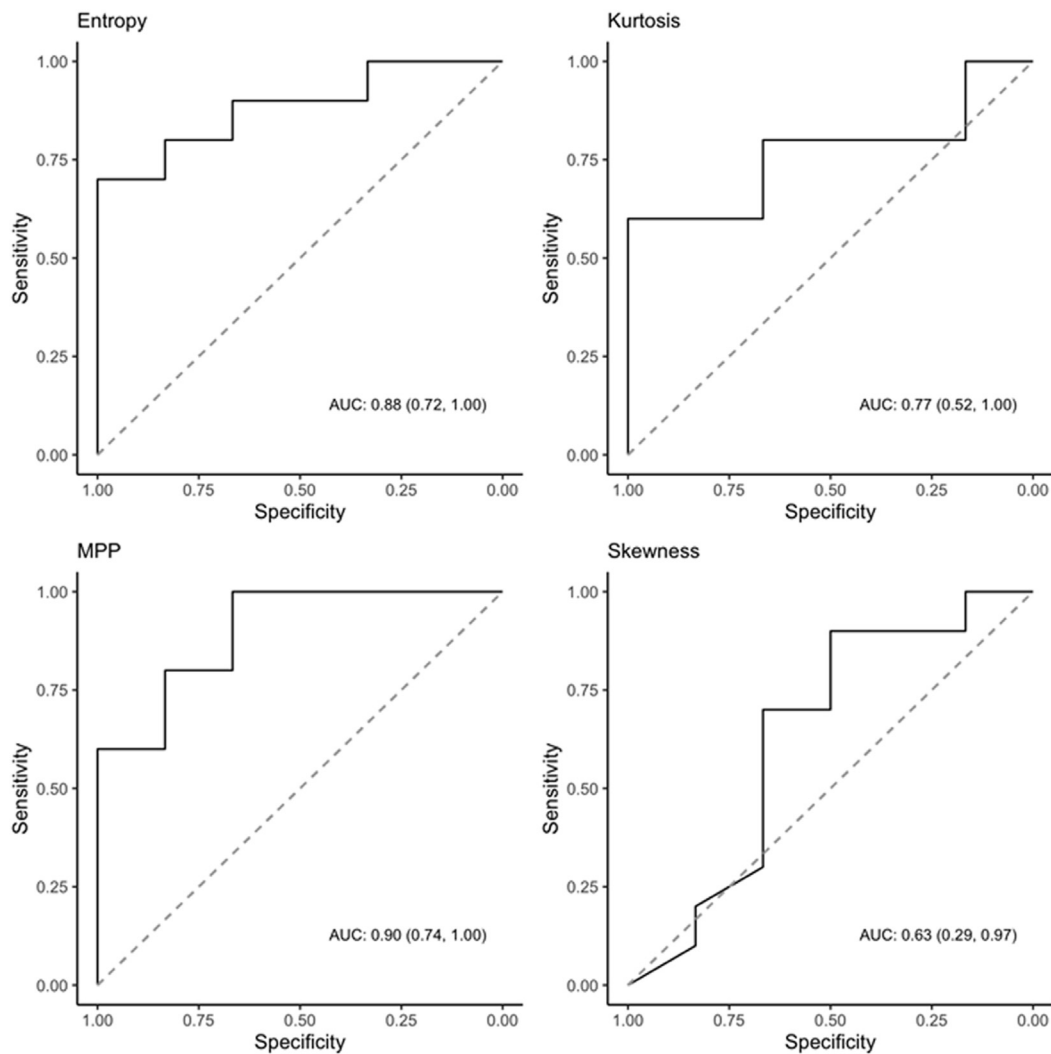


Figure 2 Receiver operator characteristic (ROC) curves of texture parameters to distinguish steatosis from NASH.

DISCUSSION

Our study shows that patients with NASH have lower mean entropy and MPP values compared to patients with simple steatosis, and that entropy and MPP cutoffs could potentially diagnose NASH with high accuracy. These findings suggest that CT texture analysis might serve as a novel imaging biomarker for disease activity that could noninvasively distinguish individuals with NASH from those with steatosis only. The importance of this findings is that the ability to identify high-risk individuals from the large number of patients with simple steatosis using non-invasive techniques, could impact management including close monitoring or intervention of patients with NASH.

NAFLD is a significant and growing public health threat as the progression to NASH can lead to cirrhosis, decompensated liver disease and hepatocellular carcinoma.^{2,3} There are currently no FDA-approved therapies for NAFLD and NASH, partially due to the lack of validated non-invasive techniques to assess hepatic steatosis, inflammation and fibrosis. In addition, easily accessible, noninvasive methods to assess hepatic inflammation and fibrosis would be useful in clinical care of patients with NAFLD to predict prognosis and to assess the response to weight loss.

While MRI-based techniques^{7,8} and CT-based attenuation measurements^{9,10} can quantify hepatic steatosis, non-invasive techniques that can detect the progression from hepatic steatosis to NASH are needed for identification of high-risk individuals. Transient elastography (FibroScan) is an ultrasound-based technique that has been utilized to assess for risk of severe fibrosis.¹⁵ However, FibroScan requires specialized equipment and can be operator dependent and is less accurate in patients with obesity. Advanced liver MR techniques, such as MR elastography or LiverMultiScan can assess fibrosis or combined inflammation and fibrosis in NAFLD, but these techniques are often more costly and require specialized equipment and processing.¹¹⁻¹⁵ Abdominal CTs are frequently performed in clinical practice and our goal was to utilize commercially available CT texture software to analyze non-contrast CT scans that are easily accessible and often obtained in the workup of other conditions. In addition, non-contrast CT has been found to be accurate in assessing hepatic steatosis across the weight spectrum, including in individuals with severe obesity.^{32,33} Of note, quantitative assessment of hepatic steatosis is traditionally performed using non-contrast CTs,^{20,21} however, recent studies have used contrast-enhanced CT including texture assessment in CTs performed in the portal-venous phase³⁴ or virtual non-contrast dual-energy CT.³⁵

CT texture analysis is a technique that determines the spatial arrangement of pixel intensities using statistical models of image intensities. CT texture analysis of the liver

has been used in patients with neoplasms to predict outcome.^{36,37} Recent studies have used CT texture analysis to assess patients with NAFLD. Dagainawala *et al.*¹⁹ utilized an in-house CT texture analysis program to evaluate and demonstrated a fair ability to differentiate between lower and higher levels of fibrosis as compared to gold standard histopathology in subjects with all types of liver disease. However, the analysis program used in the study is not commercially available, limiting its use.¹⁹ A second study compared in-house developed CT texture analysis to gold standard histopathology in 149 subjects with all types of liver disease. Fifteen texture features were analyzed averaged over 10 regions of interest per case and 4 to 7 texture features were deemed optimal to classify fibrosis with a reported accuracy rate of 67% for determination of cirrhosis versus less severe stages of hepatic fibrosis.²⁰ Naganawa *et al.* examined a group of 88 patients with NAFLD specifically and found that liver texture parameters were better at predicting NASH in patients with low suspicion for fibrosis, based on normal hyaluronic acid levels, as compared to patients with a high suspicion for fibrosis based on elevated hyaluronic acid levels.²¹ Standard texture parameters alone were poor predictors of NASH as defined by gold standard histopathology in this study.

Our study is unique in that we have an extremely well phenotyped NAFLD population with strict limitations for weight loss or weight loss surgery between the time of liver biopsy and CT. Liver biopsies were read by a single, blinded hepatopathologist. We only analyzed non-enhanced CT scans and utilized a commercially available program, TexRad, that could be uniformly utilized across different institutions. We also uniformly analyzed one filter for analysis, which is a more valid approach than utilizing data from multiple filters, as performed in prior studies.²¹ Thus, the suggestion that entropy and MPP might serve as a novel imaging biomarker for NASH versus simple steatosis from this smaller cohort is promising but requires validation in larger longitudinal studies.

The major limitation of our study includes the small sample size, which was limited due to the exclusion of subjects with weight loss surgery or more than an absolute BMI change of more than 1.5 kg/m² between the time of the CT and biopsy. Another limitation includes the time-frame of 6 months between CT and liver biopsy, however, the median time between CT and biopsy was 8 days. We have chosen the time interval of 6 months as liver histology is not expected to change if subjects maintain a stable weight, and in addition excluded subjects who demonstrated a BMI change of more than 1.5 kg/m² between the CT and biopsy.

In conclusion, unenhanced CT texture analysis might be used as a novel imaging biomarker for disease progression in NAFLD, particularly to identify individuals with NASH versus steatosis only or those with fibrosis versus no fibrosis. Additional research should be conducted on

larger cohorts explore the potential of this technology for diagnosis and monitoring of NASH and/or fibrosis.

CREDIT AUTHORSHIP CONTRIBUTION STATEMENT

Made a substantial contribution to the concept or design of the work; or acquisition, analysis or interpretation of data: L.D., A. T., N.M., K. C., J.H., S. O., M. C., E. R., K. M., M. B.

Drafted the article or revised it critically for important intellectual content: L.D., A. T., J.H., E. R., K. M., M. B.

Approved the version to be published: L.D., A. T., N.M., K. C., J.H., S. O., M. C., E. R., K. M., M. B.

All authors have participated sufficiently in the work to take public responsibility for appropriate portions of the content.

CONFLICTS OF INTEREST

LED has received research support from Pfizer (drug donation), Perspectum Ltd. (scan analysis donation) and Lumos Pharma per investigator-initiated requests and has research support from Recordati. Dr. Dichtel is a Mass General Brigham Innovation Fellow hosted by Third Rock Ventures, a venture capital firm. She remains full-time at MGH during the period of this educational program (anticipated 10/1/2022–9/30/2024). Dr. Dichtel's financial interests were reviewed and are managed by MGH and Mass General Brigham in accordance with their conflict-of-interest policies. KEC serves on the scientific advisory board for Novo Nordisk, Theratechnologies and Bristol Myers Squibb (BMS) and has received grant funding from Boehringer-Ingelheim, BMS and Novartis. KKM has received investigator-initiated grants and study medication from Amgen and study drug from Pfizer and has or recently had equity in Amgen, Bristol-Myers Squibb, General Electric, Boston Scientific, and Becton Dickinson.

ACKNOWLEDGMENTS

This work was supported by NIH K23 DK113220 (Dichtel), K24 HL092902 (Miller), and K24 DK109940 (Bredella).

FUNDING

This work was supported by NIH K23 DK113220 (Dichtel), K24 HL092902 (Miller), and K24 DK109940 (Bredella).

REFERENCES

1. Younossi ZM, Koenig AB, Abdelatif D, Fazel Y, Henry L, Wymer M. Global epidemiology of nonalcoholic fatty liver disease-Meta-analytic assessment of prevalence, incidence, and outcomes. *Hepatology*. 2016;64:73–84.
2. Adams LA, Lymp JF, St Sauver J, et al. The natural history of nonalcoholic fatty liver disease: a population-based cohort study. *Gastroenterology*. 2005;129:113–121.
3. Bugianesi E, Leone N, Vanni E, et al. Expanding the natural history of nonalcoholic steatohepatitis: from cryptogenic cirrhosis to hepatocellular carcinoma. *Gastroenterology*. 2002;123:134–140.
4. Wong RJ, Aguilar M, Cheung R, et al. Nonalcoholic steatohepatitis is the second leading etiology of liver disease among adults awaiting liver transplantation in the United States. *Gastroenterology*. 2015;148:547–555.
5. Thampanitchawong P, Piratvisuth T. Liver biopsy: complications and risk factors. *World J Gastroenterol*. 1999;5:301–304.
6. Patel V, Sanyal AJ, Sterling R. Clinical presentation and patient evaluation in nonalcoholic fatty liver disease. *Clin Liver Dis*. 2016;20:277–292.
7. Bredella MA, Ghomi RH, Thomas BJ, et al. Breath-hold 1H-magnetic resonance spectroscopy for intrahepatic lipid quantification at 3 Tesla. *J Comput Assist Tomogr*. 2010;34:372–376.
8. van Werven JR, Marsman HA, Nederveen AJ, et al. Assessment of hepatic steatosis in patients undergoing liver resection: comparison of US, CT, T1-weighted dual-echo MR imaging, and point-resolved 1H MR spectroscopy. *Radiology*. 2010;256:159–168.
9. Boyce CJ, Pickhardt PJ, Kim DH, et al. Hepatic steatosis (fatty liver disease) in asymptomatic adults identified by unenhanced low-dose CT. *AJR Am J Roentgenol*. 2010;194:623–628.
10. Pickhardt PJ, Park SH, Hahn L, Lee SG, Bae KT, Yu ES. Specificity of unenhanced CT for non-invasive diagnosis of hepatic steatosis: implications for the investigation of the natural history of incidental steatosis. *Eur Radiol*. 2012;22:1075–1082.
11. Loomba R, Cui J, Wolfson T, et al. Novel 3D magnetic resonance elastography for the noninvasive diagnosis of advanced fibrosis in NAFLD: a prospective study. *Am J Gastroenterol*. 2016;111:986–994.
12. Loomba R, Wolfson T, Ang B, et al. Magnetic resonance elastography predicts advanced fibrosis in patients with nonalcoholic fatty liver disease: a prospective study. *Hepatology*. 2014;60:1920–1928.
13. Banerjee R, Pavlides M, Tunnicliffe EM, et al. Multiparametric magnetic resonance for the non-invasive diagnosis of liver disease. *J Hepatol*. 2014;60:69–77.
14. Pavlides M, Banerjee R, Sellwood J, et al. Multiparametric magnetic resonance imaging predicts clinical outcomes in patients with chronic liver disease. *J Hepatol*. 2016;64:308–315.
15. Castera L, Friedrich-Rust M, Loomba R. Noninvasive assessment of liver disease in patients with nonalcoholic fatty liver disease. *Gastroenterology*. 2019;156:1264–1281.e4.
16. Tourassi GD. Journey toward computer-aided diagnosis: role of image texture analysis. *Radiology*. 1999;213:317–320.
17. Ganeshan B, Abaleke S, Young RC, Chatwin CR, Miles KA. Texture analysis of non-small cell lung cancer on unenhanced computed tomography: initial evidence for a relationship with tumour glucose metabolism and stage. *Cancer Imag*. 2010;10:137–143.
18. Ganeshan B, Miles KA, Young RC, Chatwin CR. Texture analysis in non-contrast enhanced CT: impact of malignancy on texture in apparently disease-free areas of the liver. *Eur J Radiol*. 2009;70:101–110.
19. Daginawala N, Li B, Buch K, et al. Using texture analyses of contrast enhanced CT to assess hepatic fibrosis. *Eur J Radiol*. 2016;85:511–517.
20. Zhang X, Gao X, Liu BJ, et al. Effective staging of fibrosis by the selected texture features of liver: which one is better, CT or MR imaging? *Comput Med Imag Graph*. 2015;46(Pt 2):227–236.

21. Naganawa S, Enooku K, Tateishi R, et al. Imaging prediction of nonalcoholic steatohepatitis using computed tomography texture analysis. *Eur Radiol*. 2018;28:3050–3058.
22. Budai BK, Toth A, Borsos P, et al. Three-dimensional CT texture analysis of anatomic liver segments can differentiate between low-grade and high-grade fibrosis. *BMC Med Imag*. 2020;20:108.
23. Lubner MG, Jones D, Kloke J, Said A, Pickhardt PJ. CT texture analysis of the liver for assessing hepatic fibrosis in patients with hepatitis C virus. *Br J Radiol*. 2019;9220180153.
24. Henson JB, Simon TG, Kaplan A, Osganian S, Masia R, Corey KE. Advanced fibrosis is associated with incident cardiovascular disease in patients with non-alcoholic fatty liver disease. *Aliment Pharmacol Ther*. 2020;51:728–736.
25. Osganian SA, Subudhi S, Masia R, et al. Expression of IGF-1 receptor and GH receptor in hepatic tissue of patients with nonalcoholic fatty liver disease and nonalcoholic steatohepatitis. *Growth Hormone IGF Res*. 2022;65101482.
26. Pantano L, Agyapong G, Shen Y, et al. Molecular characterization and cell type composition deconvolution of fibrosis in NAFLD. *Sci Rep*. 2021;1118045.
27. Kleiner DE, Brunt EM, Van Natta M, et al. Design and validation of a histological scoring system for nonalcoholic fatty liver disease. *Hepatology*. 2005;41:1313–1321.
28. Sanyal AJ, Brunt EM, Kleiner DE, et al. Endpoints and clinical trial design for nonalcoholic steatohepatitis. *Hepatology*. 2011;54:344–353.
29. Miles KA, Ganeshan B, Hayball MP. CT texture analysis using the filtration-histogram method: what do the measurements mean? *Cancer Imag*. 2013;13:400–406.
30. Tabari A, Torriani M, Miller KK, Klibanski A, Kalra MK, Bredella MA. Anorexia nervosa: analysis of trabecular texture with CT. *Radiology*. 2017;283:178–185.
31. R Core Team. *R: A Language and Environment for Statistical Computing*. Vienna, Austria: R Foundation for Statistical Computing; 2021. URL <https://www.R-project.org/>.
32. Lee SW, Park SH, Kim KW, et al. Unenhanced CT for assessment of macrovesicular hepatic steatosis in living liver donors: comparison of visual grading with liver attenuation index. *Radiology*. 2007;244:479–485.
33. Shores NJ, Link K, Fernandez A, et al. Non-contrast computed tomography for the accurate measurement of liver steatosis in obese patients. *Dig Dis Sci*. 2011;56:2145–2151.
34. Lubner MG, Graffy PM, Said A, et al. Utility of multiparametric CT for identification of high-risk NAFLD. *AJR Am J Roentgenol*. 2021;216:659–668.
35. Zhang PP, Choi HH, Ohliger MA. Detection of fatty liver using virtual non-contrast dual-energy CT. *Abdom Radiol (NY)*. 2022;47:2046–2056.
36. Brenet Defour L, Mulé S, Tenenhaus A, et al. Hepatocellular carcinoma: CT texture analysis as a predictor of survival after surgical resection. *Eur Radiol*. 2019;29:1231–1239.
37. Ravanelli M, Agazzi GM, Tononcelli E, et al. Texture features of colorectal liver metastases on pretreatment contrast-enhanced CT may predict response and prognosis in patients treated with bevacizumab-containing chemotherapy: a pilot study including comparison with standard chemotherapy. *Radiol Med*. 2019;124:877–886.

SUPPLEMENTARY DATA

Supplementary data to this article can be found online at <https://doi.org/10.1016/j.jceh.2023.04.001>.